

Steady-state dynamics and effective temperatures of quantum criticality in an open system

P. Ribeiro

*Russian Quantum Center, Novaya street 100 A, Skolkovo, Moscow area, 143025 Russia and
Centro de Física das Interações Fundamentais, Instituto Superior Técnico,
Universidade de Lisboa, Av. Rovisco Pais, 1049-001 Lisboa, Portugal*

F. Zamani

*Max Planck Institute for Physics of Complex Systems, 01187 Dresden, Germany and
Max Planck Institute for Chemical Physics of Solids, 01187 Dresden, Germany*

S. Kirchner*

Center for Correlated Matter, Zhejiang University, Hangzhou, Zhejiang 310058, China

We study the thermal and non-thermal steady state scaling functions and the steady-state dynamics of a model of local quantum criticality. The model we consider, *i.e.* the pseudogap Kondo model, allows us to study the concept of effective temperatures near fully interacting as well as weak-coupling fixed points. In the vicinity of each fixed point we establish the existence of an effective temperature –different at each fixed point– such that the equilibrium fluctuation-dissipation theorem is recovered. Most notably, steady-state scaling functions in terms of the effective temperatures coincide with the equilibrium scaling functions. This result extends to higher correlation functions as is explicitly demonstrated for the Kondo singlet strength. The non-linear charge transport is also studied and analyzed in terms of the effective temperature.

PACS numbers: 05.70.Jk, 05.70.Ln, 64.70.Tg, 72.10.Fk

The interest in understanding the dynamics of strongly correlated systems beyond the linear response regime has in recent years grown tremendously. This increased interest has largely been spurred, on the one hand, by the advancements made in controlling non-linear dynamics in engineered systems like optical traps [1, 2] and nanostructures [3–6] and, on the other hand, by the emergence of novel collective behavior in correlated bulk systems out of equilibrium [7].

The quantum dynamics in adiabatically isolated optical traps has been successfully modeled using powerful numerical schemes that build on the time-propagation of quantum states [8, 9]. In open systems, where dissipation occurs already at the equilibrium level, mainly diagrammatic techniques on the Schwinger-Keldysh contour have been employed to study the long-time limit. For nanostructured systems which allow a description of their low-energy properties in terms of a quantum impurity in contact with fermionic and/or bosonic baths, several techniques exist to describe the ensuing out-of-equilibrium properties. These approaches, however, are either perturbative in nature [10], centered around high temperatures and short times [11–15], or approximate the continuous baths by discrete Wilson chains [16, 17].

This limitation in techniques presently available to tackle quantum systems far from equilibrium should be contrasted with the anticipated richness of behavior in the non-linear regime where *e.g.* detailed balance no longer applies. The situation might be simpler for non-linear dynamics that arises in the vicinity of quantum

critical points, where a vanishing energy scale lead to scaling and universality [18–24].

For a system to reach a non-thermal steady state, time-independent ‘*dissipative*’ boundary conditions need to be present. For the case discussed here, the boundary conditions ensure a time-independent flux of particles through the system in the regime where any transient behavior will have faded away. At criticality and in the presence of such boundary conditions, one expects that the critical, *i.e.* scale-free equilibrium fluctuation spectrum will be modified for fluctuations comparable or larger than the scale set by the dissipative boundary conditions. For the dynamics near classical continuous phase transitions a well-established theoretical framework exists, tying the dynamics to the static properties and the conserved quantities of the system [25]. In addition, research established the concept of effective temperatures (T_{eff}) as a useful notion for the non-linear dynamics of classical critical systems [26, 27]. T_{eff} is commonly defined by extending the equilibrium fluctuation-dissipation theorem to the non-linear regime. The existence of effective temperatures in quantum mechanical models was recently investigated [24, 27–30] and it was established that T_{eff} can be introduced near fully interacting quantum critical points for various ‘*dissipative*’ boundary conditions [24].

In this letter we address the following general questions within a model system: Do T_{eff} exist in the vicinity of non-interacting, or weak-coupling fixed points or is their existence linked to hyperscaling? Do T_{eff} have

meaning for higher correlation functions? How unique is an effective temperature at a given fixed point once boundary conditions have been specified? Can critical scaling functions be expressed through T_{eff} and if so, how do these scaling functions relate to the equilibrium scaling functions? To address these questions it is important to choose a model with interacting and trivial fixed points that allows for a consistent treatment of the equilibrium and out-of-equilibrium physics. We introduce our model in the next section and discuss how we obtain its near and far from equilibrium properties on equal footing.

The model. We consider the pseudogap Kondo model of a magnetic impurity coupled anti-ferromagnetically to fermionic leads with a density of states that vanishes in a power-law fashion with exponent $0 \leq r \leq 1$ at their respective Fermi level, $\rho_{c,l}^-(\omega) \sim |\omega|^r \Theta(D - |\omega|)$, with half-bandwidth D ; $l = L, R$ labels the two leads, see Fig.1(a). In the multichannel version of the model the spin degree of freedom (\mathbf{S}) is generalized from $SU(2)$ to $SU(N)$ and the fermionic excitations (c) of the leads transform under the fundamental representation of $SU(N) \times SU(M)$ with N spin and M charge channels. At zero temperature (T) and $r < r_{\text{max}} < 1$, a critical point (C) separates a multichannel Kondo (MCK)-screened phase from a local moment (LM) phase at a critical value J_c of the exchange coupling $J > 0$, see Fig.1(b). The characterization of the phases and the leading power law exponents of observables of pseudogap Kondo models have been obtained by perturbative RG, large- N methods, and NRG [31–36]. Within the large- N approach, at $T = 0$, scaling arguments are able to predict the critical exponents of dynamical observables [37, 38]. Non-equilibrium steady-states (NESS) are obtained by applying a time-independent bias voltage $V = (\mu_L - \mu_R)/|e|$, where μ_l is the chemical potential of lead l , see Fig. 1(a). As T characterizes the fermionic reservoirs, it remains well-defined even for $V \neq 0$.

A similar setup has been considered in a perturbative RG-like study adapted to the NESS condition [39]. This model has also been invoked in a variational study of the dynamics following a local quench where it was found that quenches in the Kondo phase thermalize while this is not the case for quenches across the quantum critical point (QCP) into the LM regime [40]. The system is described by the Hamiltonian

$$H = \sum_{p,\alpha\sigma l} \varepsilon_{pl} c_{p\alpha\sigma l}^\dagger c_{p\alpha\sigma l} + \frac{1}{N} \sum_{ll'} \sum_{\alpha} J_{ll'} \mathbf{S}_{\alpha;l} \cdot \mathbf{s}_{\alpha;ll'}, \quad (1)$$

where $\sigma = 1, \dots, N$ and $\alpha = 1, \dots, M$ are, respectively, the $SU(N)$ -spin and $SU(M)$ -channel indices, l labels the leads and p is a momentum index. The cotunneling term [41] in Eq. (1) contains the local operators $\mathbf{s}_{\alpha;ll'}^i = \frac{1}{n_c} \sum_{pp'\sigma\sigma'} c_{p\alpha\sigma l}^\dagger t_{\sigma\sigma'}^i c_{p'\alpha\sigma' l'}$ with t the fundamental representation of $SU(N)$ and n_c is the number of fermionic single-particle states taken to be proportional to the volume of the leads and send to infinity

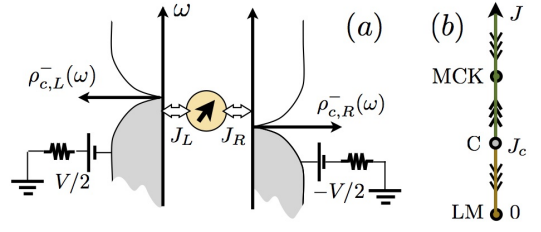


Figure 1. (a) Sketch of the model: a spin interacts with two fermionic leads which are characterized by their respective density of states $\rho_{c,L/R}^-(\omega)$ and chemical potential $\mu_{L/R}$. (b) Phase diagram of the pseudogap multichannel Kondo model with gap exponent $r < r_{\text{max}}$: A QCP (C) separates the multichannel Kondo fixed point (MCK) from the (weak-coupling) local moment fixed point (LM).

at the end of the calculation. In a totally anti-symmetric representation, one can decompose the spin operator as $S_{\sigma\sigma'} = f_{\sigma}^\dagger f_{\sigma'} - q \delta_{\sigma\sigma'}$, where q is subject to the constraint $\hat{Q} = \sum_{\sigma} f_{\sigma}^\dagger f_{\sigma} = qN$ and the $f_{\sigma}^\dagger, f_{\sigma}$ obey fermionic commutation relations.

We employ a dynamical large- N limit [37, 42], suitably generalized to the Keldysh contour [23, 24] while keeping $q = \frac{Q}{N}$ and $\kappa = M/N$ constant. This results in

$$\Sigma_B^{>,<}(t) = iG_f^{>,<}(t) G_c^{<,>}(-t) \quad (2)$$

$$\Sigma_f^{>,<}(t) = -i\kappa G_B^{>,<}(t) G_c^{>,<}(t) \quad (3)$$

$$-iG_f^{<}(t) = q, \quad (4)$$

where G_f is the pseudofermion propagator and G_B is the propagator of a bosonic Hubbard-Stratonovich decoupling field. Σ_f (Σ_B) is the proper selfenergy of G_f (G_B) and is related to it via the Dyson equation. For details see Ref. [46]. We assume that the exchange interaction originates from an Anderson-type model via a Schrieffer-Wolff transformation, so that a single coupling constant $J = J_L + J_R$ emerges [46].

The set of self-consistent equations for the lesser and larger components of G_f and G_B were solved numerically on a discrete logarithmic frequency grid [46]. In equilibrium, our approach yields dynamical scaling functions that coincide with those obtained from quantum Monte-Carlo [43]. Most importantly for the questions pursued here, it treats thermal and non-thermal steady states on equal footing.

Observables. The critical point (C) is beyond the Ginzburg-Landau-Wilson paradigm, yet a possible order parameter for the transition from the overscreened Kondo to local-moment phase is given by $\lim_{T \rightarrow 0} T \chi(\omega = 0, T)$, where $\chi(\omega, T)$ is the Fourier transform of the local (impurity) spin-spin correlation function $\chi(t - t')$, see Fig. 2(a).

We work on the Keldysh contour where the lesser and greater components are defined in the usual way as $\chi^{>}(t - t') = -i \frac{1}{N} \sum_a \langle S^a(t) S^a(t') \rangle$ with $t \in \gamma_{\leftarrow}$ and $t' \in \gamma_{\rightarrow}$ and $\chi^{<}(t - t') = -i \frac{1}{N} \sum_a \langle S^a(t') S^a(t) \rangle$,

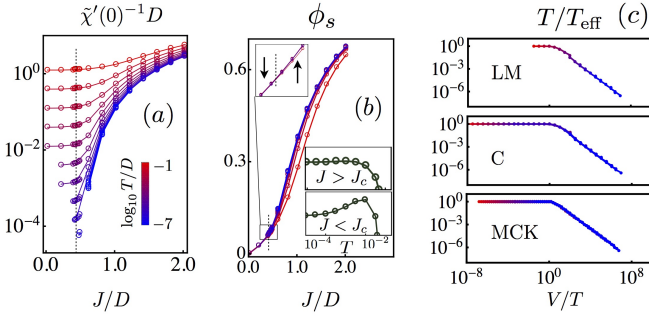


Figure 2. (a) Inverse of the static spin susceptibility as a function of J for different temperatures. (b) Singlet-strength as a function of J plotted for different values of the temperature. The inset shows that, as temperature decreases, the $T = 0$ curve is approached from below in the MCK and from above in the LM phases. (c) Scaling T_{eff}/T vs V/T : intermediate (MCK and C) and weak coupling fixed point (LM) show $T_{\text{eff}} \sim V$ for $V \gg T$.

with $t \in \gamma_{\rightarrow}$ and $t' \in \gamma_{\leftarrow}$ so that $\chi^R(t) = \Theta(t)[\chi^>(t) - \chi^<(t)]$ and $\chi^A = \chi^R + \chi^< - \chi^>$. Here, $\gamma_{\rightarrow(\leftarrow)}$ is the forward (backward) branch of the Keldysh contour, respectively.

We also consider the “singlet-strength” ϕ_s , which we define through the Kondo term contribution to the total energy of the system as $\frac{1}{N} \sum_{ll'} \sum_c J_{ll'} \langle \mathbf{S} \cdot \mathbf{s}_{c, ll'} \rangle = -J\kappa \left(\frac{N^2 - 1}{N} \right) \phi_s$. In this way, ϕ_s is a dimensionless quantity, which possesses a well-defined large- N limit and quantifies the degree of singlet formation. In terms of the fermionic fields, it can be written as the local-in-time limit of a 4-point correlator [46]. The equilibrium properties of this novel quantity will be discussed below. The steady state charge current passing through each channel is $\mathcal{J}_P = -\partial_t \langle \hat{N}_L(t) \rangle / M$, where $\hat{N}_L = \sum_{p\alpha\sigma} c_{p\alpha\sigma L}^\dagger c_{p\alpha\sigma L}$ is the number of particles in the left lead. The out-of-equilibrium conditions considered here respect particle-hole symmetry which implies a vanishing energy current.

We now turn to a discussion of our results. Throughout the paper we set $\kappa = 0.3$, $r = 0.2$, and $q = 1/2$. This results in $r_{\text{max}} = 0.412(4)$. Our choice of values for κ and r ensures a finite static spin susceptibility $\chi'(\omega = 0)$ within the MCK phase as $T \rightarrow 0$.

Thermal steady-state. The equilibrium ($V = 0$) behavior of $\chi'(\omega = 0, T)$ in the relaxational regime ($\omega \ll T$) near the MCK, C, and LM fixed points is shown in Fig.2-(a). For $J < J_c \simeq 0.44D$, i.e. in the LM phase, one observes Curie-like behavior at lowest temperatures $\chi'(\omega = 0, T) \propto T^{-1}$. In the MCK phase ($J > J_c$ and with our choices of κ and r), the $T = 0$ susceptibility remains finite. The grey lines in Figs.3-(b) show the scaling plots of the logarithmic derivative of $\chi''(\omega)$ for different values of the temperature, i.e. $\partial_{\ln \omega} \ln \chi''(\omega) \simeq \alpha_\chi$ within the scaling region where $\chi''(\omega) \propto |\omega|^{\alpha_\chi}$. The values of α_χ

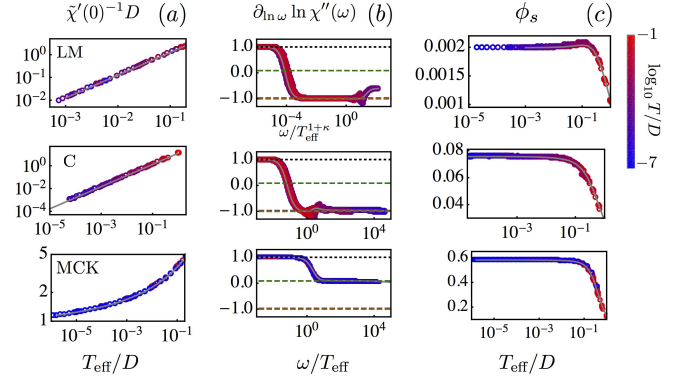


Figure 3. Scaling of different observables with T_{eff} at different fixed points: (a) Inverse static susceptibility $\chi'(0)^{-1}$ vs T_{eff} ; (b) $\partial_{\ln \omega} \ln \chi''(\omega)$ vs ω/T_{eff} ; (c) singlet strength ϕ_s vs T_{eff} . For each fixed point, the equilibrium scaling form (grey lines) is compared with the same quantity under non-equilibrium conditions and T substituted by T_{eff} .

in the quantum coherent regime ($\omega/T \gg 1$) agree with those obtained analytically from a $T = 0$ scaling ansatz [38] for the MCK ($\alpha_\chi \simeq 0.087$) and C ($\alpha_\chi = -0.97$) fixed points. These results are compatible with a dynamical scaling form $\chi''(\omega, T) = T^{\alpha_\chi} \Phi(\omega/T)$, in terms of an universal scaling function $\Phi(x)$ possessing asymptotic values $\Phi(x) \propto x$ for $x \ll 1$ and $\Phi(x) \propto x^{\alpha_\chi}$ for $x \gg 1$. Thus, the scaling properties are in line with dynamical ω/T -scaling for the C and MCK fixed points. For the LM fixed point we find $\alpha_\chi = -1$ and a scaling form $\chi''(\omega) = T^{\alpha_\chi} \tilde{\Phi}(\omega/T^{1+\kappa})$, indicative of a weak-coupling fixed point and absence of hyperscaling. These results will be further addressed elsewhere [38].

The singlet-strength ϕ_s vs. J at different T and at $V = 0$ is shown in Fig.2-(b). The numerical data at $T \neq 0$ suggest that $\phi_s(J, T = 0)$ is a continuous function of J . Fig.2-(b) shows that the way the $T \rightarrow 0$ limit is approached is distinct within the two phases: $\phi_s(J, T) - \phi_s(J, T \rightarrow 0) > 0$ for the LM and $\phi_s(J, T) - \phi_s(J, T \rightarrow 0) < 0$ in the MCK phases. At the C fixed point we find that $\phi_s(J, T)$ as a function of J crosses for different values of T (for sufficiently low T).

Non-thermal steady-states. We consider a non-equilibrium setup where the two leads, initially decoupled from the impurity (for $t < t_0$), are held at chemical potentials $\mu_L = -\mu_R = |e|V/2$ ($|e| = 1$ in the following). At $t = t_0$ the coupling between the leads and the impurity is turned on. A steady-state is reached by sending $t_0 \rightarrow -\infty$ so that any transient behavior will already have faded away at (finite) time t . The NESS fluctuation-dissipation ratio (FDR) for a dynamical observable $A(t, t') = A(t - t')$ is defined through $\text{FDR}_A(\omega) = [A^>(\omega) + A^<(\omega)]/[A^>(\omega) - A^<(\omega)]$, where $A^>(<)$ are the Fourier transforms of the greater/lesser components of A . At equilibrium, the fluctuation-

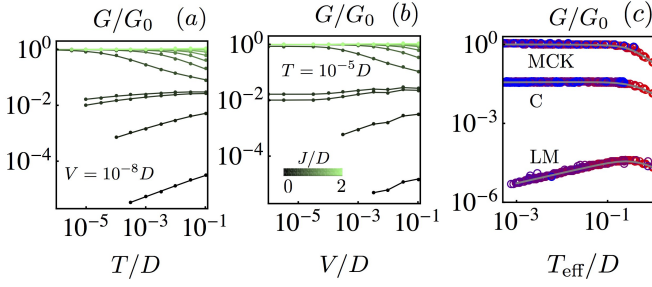


Figure 4. Conductance G normalised to the MCK fixed point conductance G_0 . (a) $G(T)$ as a function of temperature computed for the lowest non-zero value of V for several values of J (see color coding). (b) G as a function of the bias voltage for fixed temperature. (c) $G = \mathcal{J}_P/V$ vs T_{eff} at different fixed points. The equilibrium form is given by the grey lines.

dissipation theorem implies $\text{FDR}_A(\omega) = \tanh(\beta\omega/2)^\zeta$ uniquely (with $\zeta = \pm 1$ for fermionic (+) and bosonic (-) operators). For a generic out-of-equilibrium system, the functional form of the FDR differs from the equilibrium one. A frequency-dependent “effective temperature”, $1/\beta_{\text{eff}}^A(\omega)$, for the observable A can be defined by requiring that $\tanh[\beta_{\text{eff}}^A(\omega)\omega/2] = \text{FDR}_A(\omega)$ [29, 44]. Following Refs. [24, 26, 28] we define T_{eff} via FDR_χ through its asymptotic low-frequency behavior $T_{\text{eff}}^{-1} = \lim_{\omega \rightarrow 0} \beta_{\text{eff}}^\chi(\omega)$. Clearly, in equilibrium $T_{\text{eff}} = T$. On the other hand, a linear-in- V decoherence rate in the non-equilibrium relaxational regime near an interacting quantum critical point is signaled by ω/V -scaling [23]. Thus, in this case and at $T = 0$ one expects $T_{\text{eff}} = cV$, where c characterizes the underlying fixed point. This has been explicitly demonstrated in Ref. 20. Therefore, it is reasonable to expect that analyzing T_{eff}/T vs V/T will bring out the universal factor c , which is indeed what we find: Fig. 2-(c) shows the resulting T_{eff}/T as a function of V/T for the different fixed points computed for different values of V and T . In the non-linear regime, the scaling collapse for T_{eff}/T implies $T_{\text{eff}} = cV$, where $1/c$ is the amplitude of the scaling curve in the non-linear regime. Note that even for the LM fixed point, where hyperscaling is violated, $T_{\text{eff}} \sim V$ holds for $V \gg T$, see Fig. 2-(c), top panel. We checked that different values of J within the LM and the MCK phases result in the same T_{eff}/T vs V/T_{eff} curve for sufficiently low temperature T .

Far from equilibrium and outside any scaling regime, χ is a function of ω , T , and V but near a fixed point $\chi(\omega, T, V)$ develops a scaling form in terms of a combination of ω , T , and V . This then raises the question how T_{eff} enters the scaling function and leads us to a remarkable result, see Fig. 3-(b)-(c): The non-thermal steady-state scaling function of $\chi = \chi(\omega, T, V)$ when scaled in terms of T_{eff} recovers the equilibrium scaling function of that particular fixed point with T_{eff} replacing T . This not only turns out to be true for χ at each of the fixed points of the

model but also holds for the singlet-strength, a higher-order correlation function, as will be demonstrated. We first consider the static susceptibility. Fig. 3-(a) shows the equilibrium scaling forms of $\chi'(0)^{-1}$ as a function of T_{eff} for different values of temperature and bias voltage V for the LM, C and MCK fixed points. The color coding reflects the values of temperature T of the system. The equilibrium form (grey lines) is recovered even for $T_{\text{eff}}/T \gg 1$.

A similar result can be obtained at finite ω : Fig. 3-(b) shows the log-derivative $\partial_{\ln \omega} \ln \chi''(\omega)$ as a function of ω/T_{eff} for different values of T and V for the LM, C and MCK fixed points. These should be compared with the equilibrium results, the underlying grey lines: The equilibrium scaling form is recovered by replacing T by T_{eff} . Note that T_{eff} is defined from the FDR of the susceptibility in the limit $\omega/T \rightarrow 0$. Therefore, the fact that the equilibrium scaling forms of $\chi'(0)$ and $\chi''(\omega)$ are reproduced for $T_{\text{eff}}/T \gg 1$ and $\omega/T_{\text{eff}} \gg 1$, respectively, is remarkable. Fig. 3-(c) depicts ϕ_s as a function of T_{eff} for different values of T and V . Again, the equilibrium scaling behavior (gray lines) is reproduced.

We now turn to the discussion of the charge current. Unlike χ and ϕ_s , the conductance G depends on both pseudoparticle propagators G_f & G_B . One thus may wonder if T_{eff} can have any meaning for G . In Figs. 4-(a,b) we show the conductance per channel $G = \mathcal{J}_P/V$ vs T and V respectively. In the linear response regime $V, T \ll T_K(J)$ of the MCK phase, the current is proportional to the applied voltage $\mathcal{J}_P = G_0 V$. Outside of the scaling regime, i.e. for $V, T \gg T_K(J)$, G drops rapidly as V or T increase. $G_0 h \simeq 0.415$ is the universal analog for the multichannel case of the unitary limit of the $SU(2)$ Kondo model. The linear and non-linear current-voltage characteristics display power-law behavior as $T, V \rightarrow 0$ [23, 24]. Near C, i.e. for $J = J_c$, the relation between the current and the applied voltage is still linear, ($\mathcal{J}_P = G_c V$), however the critical conductance G_c is much smaller than G_0 . Fig. 4-(c) shows the conductance G as a function of T_{eff} for different values of T and V for the LM, C and MCK fixed points. The grey lines are obtained by varying the temperature at fixed V for the lowest value of V considered in our study, i.e. $V_{\text{min}} = 10^{-8}D$. The results are remarkable as the temperature dependence of the linear response conductance is reproduced at all fixed points when the non-linear conductance is taken as a function of T_{eff} . This is true even for values of V several orders of magnitude larger than V_{min} .

In conclusion, we have addressed the steady-state dynamics near quantum critical points and analyzed it in terms of effective temperatures. We found that both weak and intermediate coupling fixed points can be characterized by an T_{eff} and that all observables studied (χ, ϕ_s, G) scale in terms of the same T_{eff} within the scaling regime. Even more surprisingly, at all fixed points,

the local spin-spin correlation function χ and the singlet-strength ϕ_s assume their equilibrium scaling functions even far from equilibrium when scaled in terms of T_{eff} , *i.e.* T_{eff} replacing T . A similar result relates the linear and non-linear conductance. We note that in the (non-interacting) pseudogap resonant level model such behavior is absent [38]. Non-equilibrium current noise near quantum criticality in systems possessing a gravity dual appears thermal [45]. Our results imply that similar results hold for a larger class of quantum critical systems and quantities. To which extend our results rely on locality needs to be further investigated. We note, however, that the type of models considered here are relevant to the DMFT approach to lattice systems out of equilibrium [14].

Acknowledgments. Helpful discussions with K. Ingersent, A. Mitra, and Q. Si are gratefully acknowledged. P. Ribeiro was supported by the Marie Curie International Reintegration Grant PIRG07-GA-2010-268172. S. Kirchner acknowledges partial support by the National Natural Science Foundation of China, grant No.11474250.

* stefan.kirchner@correlated-matter.com

- [1] T. Kinoshita, T. Wenger, and D. S. Weiss, *Nature* **440**, 900 (2006).
- [2] I. Bloch and W. Zwerger, *Rev. Mod. Phys.* **80**, 885 (2008).
- [3] M. Grobis, I. G. Rau, R. M. Potok, H. Shtrikman, and D. Goldhaber-Gordon, *Phys. Rev. Lett.* **100**, 246601 (2008).
- [4] G. D. Scott, D. Natelson, S. Kirchner, and E. Muñoz, *Phys. Rev. B* **87**, 241104 (2013).
- [5] L. L. Bonilla and H. T. Grahn, *Rep. Prog. Phys.* **68**, 577 (2005).
- [6] J. Dubois, T. Jullien, F. Portier, P. Roche, A. Cavanna, Y. Jin, W. Wegscheider, P. Roulleau, and D. C. Glatli, *Nature* **502**, 659 (2013).
- [7] R. Mankowsky, A. Subedi, M. Först, S. O. Mariager, M. Cholle, H. Lemke, J. Robinson, J. Glownia, M. Minitti, A. Frano, et al., *Nature* **516**, 71 (2014).
- [8] M. Eckstein, A. Hackl, S. Kehrein, M. Kollar, M. Moeckel, P. Werner, and F. Wolf, *The European Physical Journal Special Topics* **180**, 217 (2010).
- [9] E. Arrigoni, M. Knap, and W. von der Linden, *Phys. Rev. Lett.* **110**, 086403 (2013).
- [10] E. Muñoz, C. J. Bolech, and S. Kirchner, *Phys. Rev. Lett.* **110**, 016601 (2013).
- [11] P. Werner, T. Oka, and A. Millis, *Phys. Rev. B* **79**, 035320 (2009).
- [12] E. Gull, D. R. Reichman, and A. J. Millis, *Phys. Rev. B* **84**, 085134 (2011).
- [13] G. Cohen, E. Gull, D. R. Reichman, A. J. Millis, and E. Rabani, *Phys. Rev. B* **87**, 195108 (2013).
- [14] H. Aoki, N. Tsuji, M. Eckstein, M. Kollar, T. Oka, and P. Werner, *Rev. Mod. Phys.* **86**, 779 (2014).
- [15] M. Schiró and M. Fabrizio, *Phys. Rev. Lett.* **105**, 076401 (2010).
- [16] A. Rosch, *Eur. Phys. J. B* **85**, 6 (2012).
- [17] H. T. M. Nghiem and T. A. Costi, *Phys. Rev. B* **90**, 035129 (2014).
- [18] S. Diehl, A. Micheli, A. Kantian, B. Kraus, H. P. Büchler, and P. Zoller, *Nature Phys.* **4**, 878 (2008).
- [19] L. M. Sieberer, S. D. Huber, E. Altman, and S. Diehl, *Phys. Rev. Lett.* **110**, 195301 (2013).
- [20] A. Mitra, S. Takei, Y. B. Kim, and A. J. Millis, *Phys. Rev. Lett.* **97**, 236808 (2006).
- [21] S. Takei, W. Witczak-Krempa, and Y. B. Kim, *Phys. Rev. B* **81**, 125430 (2010).
- [22] C.-H. Chung, K. Le Hur, M. Vojta, and P. Wölfle, *Phys. Rev. Lett.* **102**, 216803 (2009).
- [23] S. Kirchner and Q. Si, *Phys. Rev. Lett.* **103**, 206401 (2009).
- [24] P. Ribeiro, Q. Si, and S. Kirchner, *Europhys. Lett.* **102**, 50001 (2013).
- [25] P. C. Hohenberg and B. I. Halperin, *Rev. Mod. Phys.* **49**, 435 (1977).
- [26] P. Hohenberg and B. I. Shariman, *Physica D: Nonlinear Phenomena* **37**, 109 (1989).
- [27] L. F. Cugliandolo, J. Kurchan, and L. Peliti, *Phys. Rev. E* **55**, 3898 (1997).
- [28] A. Mitra and A. J. Millis, *Phys. Rev. B* **72**, 1 (2005).
- [29] S. Kirchner and Q. Si, *phys. stat. sol. b* **247**, 631 (2010).
- [30] A. Caso, L. Arrachea, and G. S. Lozano, *Phys. Rev. B* **83**, 1 (2011).
- [31] D. Withoff and E. Fradkin, *Phys. Rev. Lett.* **64**, 1835 (1990).
- [32] C. Gonzalez-Buxton and K. Ingersent, *Phys. Rev. B* **57**, 14254 (1998).
- [33] D. E. Logan and M. T. Glossop, *J. Phys.: Condens. Matter* **12**, 985 (2000).
- [34] L. Fritz, S. Florens, and M. Vojta, *Phys. Rev. B* **74**, 144410 (2006).
- [35] R. Bulla, T. Pruscke, and A. Hewson, *J. Phys.: Condens. Matter* **9**, 10463 (1997).
- [36] K. Ingersent and Q. Si, *Phys. Rev. Lett.* **89**, 076403 (2002).
- [37] M. Vojta, *Phys. Rev. Lett.* **87**, 097202 (2001).
- [38] F. Zamani, P. Ribeiro, and S. Kirchner, (unpublished) (2015).
- [39] C.-H. Chung and K. Y.-J. Zhang, *Phys. Rev. B* **85**, 195106 (2012).
- [40] M. Schiró, *Phys. Rev. B* **86**, 161101 (2012).
- [41] A. Kaminski, Y. Nazarov, and L. I. Glazman, *Physical Review B* **62**, 8154 (2000).
- [42] O. Parcollet, A. Georges, G. Kotliar, and A. Sengupta, *Phys. Rev. B* **58**, 3794 (1998).
- [43] M. T. Glossop, S. Kirchner, J. Pixley, and Q. Si, *Phys. Rev. Lett.* **107**, 076404 (2011).
- [44] L. Foini, L. Cugliandolo, and A. Gambassi, *Phys. Rev. B* **84**, 1 (2011).
- [45] J. Sonner and A. G. Green, *Phys. Rev. Lett* **109**, 091601 (2012).
- [46] See Supplementary Material.

Steady-state dynamics and effective temperatures of quantum criticality in an open system: Supplementary Material

P. Ribeiro,^{1,2} F. Zamani,^{3,4} and S. Kirchner⁵

¹*Russian Quantum Center, Novaya street 100 A, Skolkovo, Moscow area, 143025 Russia*

²*Centro de Física das Interações Fundamentais, Instituto Superior Técnico, Universidade de Lisboa, Av. Rovisco Pais, 1049-001 Lisboa, Portugal*

³*Max Planck Institute for Chemical Physics of Solids, Nöthnitzer Straße 40, 01187 Dresden, Germany*

⁴*Max Planck Institute for the Physics of Complex Systems, Nöthnitzer Straße 38, 01187 Dresden, Germany*

⁵*Center for Correlated Matter, Zhejiang University, Hangzhou, Zhejiang 310058, China*

Generating functional on the Keldysh contour

The generating functional on the Keldysh contour can be written as

$$\begin{aligned} Z[\xi] = & \int Dc \int Df \int D\lambda e^{i(c^\dagger g_c^{-1} c + f^\dagger g_f^{-1} f)} e^{iqN \int_\gamma dz \lambda_z} \\ & \times e^{+i\frac{1}{N} \int_\gamma dz \sum_\alpha J_{ll'z} (\sum_\sigma f_{\sigma,z}^\dagger c_{0,\alpha\sigma l'z}) (\sum_{\sigma'} c_{0\alpha\sigma' lz}^\dagger f_{\sigma'z})} \\ & \times e^{c^\dagger \xi_c + \xi_c^\dagger c + f^\dagger \xi_f + \xi_f^\dagger f} \end{aligned} \quad (\text{S.1})$$

where ξ_c and ξ_f act as sources to the fermionic c and f fields and λ is a scalar Lagrange multiplier enforcing the constraint $\sum_\sigma f_{\sigma z}^\dagger f_{\sigma z} = qN$. $\int_\gamma dz$ is the integral over the Keldysh contour $\gamma = \gamma_{\rightarrow} + \gamma_{\leftarrow}$ with its forward (γ_{\rightarrow}) and backward (γ_{\leftarrow}) branches.

Here, the inverse bare propagators are

$$g_f^{-1} = (i\partial_z - \lambda_z), \quad (\text{S.2})$$

$$g_c^{-1} = (i\partial_z - \varepsilon_{pl}). \quad (\text{S.3})$$

In analogy to the equilibrium procedure –albeit performed on the Matsubara contour– one can introduce a Hubbard-Stratonovich decoupling field $B_{\alpha lz}$ conjugated to $\sum_{\sigma'} c_{0\alpha\sigma' lz}^\dagger f_{\sigma' z}$, to decouple the quartic fermionic term in Eq.(S.1). Thus,

$$\begin{aligned} Z[\xi] = & \int Df \int D\lambda \int DB e^{i(f^\dagger g_f^{-1} f)} e^{i \int dz \lambda_z Q} e^{i(B_{\alpha}^\dagger g_B^{-1} B_{\alpha})} \\ & \times e^{-i\frac{1}{N} \int dz \int dz' \sum_{\sigma\alpha l} B_{\alpha lz} B_{\alpha lz'}^\dagger \tilde{g}_{c,l}(z, z') f_{\sigma,z}^\dagger f_{\sigma,z'}} \\ & \times e^{\left[-\frac{1}{\sqrt{N}} \int_\gamma dz' \sum_{\alpha'\sigma'} (\xi_c^\dagger g_c)_{0\alpha'\sigma' l' z} B_{\alpha l' z'}^\dagger f_{\sigma' z'} - \frac{1}{\sqrt{N}} \int_\gamma dz \sum_{\sigma\alpha} f_{\sigma,z}^\dagger B_{\alpha lz} (g_c \cdot \xi_c)_{0\alpha\sigma lz}\right]} \\ & \times e^{i\xi_c^\dagger g_c \xi_c} e^{f^\dagger \xi_f + \xi_f^\dagger f} \end{aligned} \quad (\text{S.4})$$

with

$$g_{B;ll'}^{-1} = -\left[\tilde{J}^{-1}\right]_{ll'}, \quad (\text{S.5})$$

where $\left[\tilde{J}\right]_{ll'} = J_{ll'}$, is the bare inverse propagator of the B field.

Finally, with the help of the complex-valued dynamic Hubbard-Stratonovich fields $W_{zz';l}$ one obtains

$$\begin{aligned} Z[\xi] = & \int D\lambda \int DW e^{N \text{tr} \ln[-iG_f^{-1}] - M \text{tr} \ln[-i(G_B^{-1} + V_{\xi_c}^\dagger G_f V_{\xi_c})]} \\ & e^{iN \text{tr}[W^\dagger * [\tilde{g}_c]^{-1} * W] + i \int dz \lambda_z Q} \\ & e^{-i\xi_f^\dagger G_f V_{\xi_c} [G_B^{-1} + V_{\xi_c}^\dagger G_f V_{\xi_c}]^{-1} V_{\xi_c}^\dagger G_f \xi_f + i\xi_c^\dagger g_c \xi_c + i\xi_f^\dagger G_f \xi_f} \end{aligned} \quad (\text{S.6})$$

with

$$G_f^{-1}(z, z') = g_f^{-1}(z, z') - W_{zz';l} \quad (\text{S.7})$$

$$G_B^{-1}(z, z') = g_b^{-1}(z, z') - \bar{W}_{z'z;l} \quad (\text{S.8})$$

$$\text{tr} \left[W^\dagger * [\tilde{g}_c]^{-1} * W \right] = \sum_l \int dz \int dz' \frac{\bar{W}_{zz';l} W_{zz';l}}{\tilde{g}_{c,l}(z, z')} \quad (\text{S.9})$$

and $V_{\xi_c}^\dagger$ and V_{ξ_c} are source-dependent terms. Eq.(S.6) is used to derive all correlators by taking derivatives with respect to the source fields.

Dynamical large-N self-consistency equations on the Keldysh contour

In this section we set the sources to zero and compute the saddle-point equations with respect to the bosonic fields W and λ . The generating functional in the absence of sources is

$$Z[\xi = 0] = \int D\lambda \int DW e^{iN S[W, \lambda]} \quad (\text{S.10})$$

with

$$S[W, \lambda] = q \int dz \lambda_z + \text{tr} [W^\dagger * [\tilde{g}_c]^{-1} * W] - i \frac{1}{N} \text{tr} \ln [-iG_f^{-1}] + i\kappa \frac{1}{M} \text{tr} \ln [-iG_B^{-1}]. \quad (\text{S.11})$$

The saddle point equations are obtained by putting the linear variation of $S[W, \lambda]$ with respect to W and λ to zero:

$$\frac{\delta}{\delta W_{zz',l}} S[W, \lambda] = \bar{W}_{zz',l} [\tilde{g}_c(z, z')]^{-1} + i \frac{1}{N} \sum_\sigma G_f(z', z) = 0, \quad (\text{S.12})$$

$$\frac{\delta}{\delta \bar{W}_{zz',l}} S[W, \lambda] = [\tilde{g}_{c,l}(z, z')]^{-1} W_{zz',l} - i\kappa \frac{1}{M} \sum_\alpha G_{B;ll}(z, z') = 0, \quad (\text{S.13})$$

$$\frac{\delta}{\delta \lambda_z} S[W, \lambda] = q + i \frac{1}{N} \sum_\sigma G_f(z^-, z) = 0. \quad (\text{S.14})$$

These equations become *exact* in the large-N limit. These equations are equivalent to

$$\begin{aligned} \hat{G}_f^{-1} &= \hat{g}_f^{-1} - \Sigma_f \\ \hat{G}_B^{-1} &= \hat{g}_B^{-1} - \Sigma_B \\ q &= -i\hat{G}_f(z^-, z) \end{aligned}$$

with

$$\Sigma_B(z, z') = \begin{pmatrix} \bar{W}_{z'z,L} & 0 \\ 0 & \bar{W}_{z'z,R} \end{pmatrix} = -i \begin{pmatrix} \tilde{g}_{c,L}(z', z) & 0 \\ 0 & \tilde{g}_{c,R}(z', z) \end{pmatrix} \hat{G}_f(z, z') \quad (\text{S.15})$$

$$\Sigma_f(z, z') = \delta_{\sigma\sigma'} \sum_l W_{zz',l} = \delta_{\sigma\sigma'} i\kappa \sum_l \tilde{g}_{c,l}(z, z') \hat{G}_{B;ll}(z, z'). \quad (\text{S.16})$$

Note that λ_z evaluated at the saddle-point is time independent, *i.e.* $\lambda_t = \lambda$.

Singular exchange coupling matrix J

So far, the treatment has been general and no particular form of the Kondo exchange coupling matrix has been assumed. For the physically most relevant case where the Kondo Hamiltonian is derived from an Anderson-type model through a Schrieffer-Wolff transformation, the exchange matrix $J_{ll'}$ ($l, l' = L, R$) takes the form

$$J = \begin{pmatrix} J_L & \sqrt{J_L J_R} \\ \sqrt{J_L J_R} & J_R \end{pmatrix}.$$

Thus, the exchange coupling matrix is singular, $\det(J) = 0$. In this case, where one of the eigenvalues of J vanishes, we can write

$$\tilde{J} = |u_+\rangle (J_L + J_R) \langle u_+|$$

with

$$\begin{aligned} |u_-\rangle &= -\sqrt{\frac{J_R}{J_L + J_R}} |L\rangle + \sqrt{\frac{J_L}{J_L + J_R}} |R\rangle \\ |u_+\rangle &= \sqrt{\frac{J_L}{J_L + J_R}} |L\rangle + \sqrt{\frac{J_R}{J_L + J_R}} |R\rangle. \end{aligned}$$

As the exchange matrix is singular, the component u_- of the B field has to vanish and thus

$$\hat{G}_B = |u_+\rangle \hat{G}_{B+} \langle u_+|.$$

In this case the self-consistent equations simplify to

$$\Sigma_{B+}(z, z') = -i\tilde{g}_{c,+}(z', z)\hat{G}_f(z, z'), \quad (\text{S.17})$$

$$\Sigma_f(z, z') = i\kappa\tilde{g}_{c,+}(z, z')\hat{G}_{B+}(z, z'), \quad (\text{S.18})$$

with

$$\begin{aligned} \hat{G}_{B+}^{-1} &= \hat{g}_{B+}^{-1} - \Sigma_B, \\ \hat{g}_{B+}^{-1} &= \frac{-1}{J_L + J_R}, \\ \tilde{g}_{c,+} &= \frac{J_L\tilde{g}_{c,L} + J_R\tilde{g}_{c,R}}{J_L + J_R}. \end{aligned}$$

Using Langreth's rules, we obtain

$$\Sigma_B^{>,<}(t, t') = -i\tilde{g}_c^{<,>}(t', t)\hat{G}_f^{>,<}(t, t'), \quad (\text{S.19})$$

$$\Sigma_f^{>,<}(t, t') = i\kappa\tilde{g}_c^{>,<}(t, t')\hat{G}_B^{>,<}(t, t'), \quad (\text{S.20})$$

$$q = -i\hat{G}_f^{<}(0). \quad (\text{S.21})$$

Non-equilibrium steady-state (NESS) description

The steady-state condition implies that the system is time translationally invariant so that $G^{R,A,K}(t, t') = G^{R,A,K}(t - t')$. Therefore, it is advantageous to solve the self-consistent equations in the frequency domain. The conventions of the Fourier transform used by us are

$$\begin{aligned} A(t) &= \int \frac{d\omega}{2\pi} A(\omega) e^{-i\omega t}, \\ A(\omega) &= \int dt A(t) e^{i\omega t}. \end{aligned}$$

Eq.(S.19-S.21) take the form

$$\Sigma_B^{>,<}(\omega) = -i \int \frac{d\nu}{2\pi} \tilde{g}_c^{<,>}(\nu - \omega) G_f^{>,<}(\nu), \quad (\text{S.22})$$

$$\Sigma_f^{>,<}(\omega) = i\kappa \int \frac{d\nu}{2\pi} \tilde{g}_c^{>,<}(\omega - \nu) G_B^{>,<}(\nu), \quad (\text{S.23})$$

$$q = -i \int \frac{d\omega}{2\pi} G_f^{<}(\omega). \quad (\text{S.24})$$

The reservoirs are in equilibrium and are thus characterized by their respective chemical potentials μ_L and μ_R and their respective temperatures $T_L = T_R = T$. We introduce the following reservoir quantities

$$\rho_{c,l}^{\pm}(\omega) = -\frac{1}{2\pi i} \left[\tilde{g}_{c,l}^{>}(\omega) \pm \tilde{g}_{c,l}^{<}(\omega) \right], \quad (\text{S.25})$$

$$\rho_{c,l}^H(\omega) = -\frac{1}{\pi} P \int d\nu \frac{\rho_{c,l}^-(\nu)}{\omega - \nu}, \quad (\text{S.26})$$

where $\rho_{c,l}^-(\omega) = \frac{1}{L} \sum_p \delta(\omega - \varepsilon_{pl})$ is the normalized ($\int d\omega \rho_{c,l}^-(\omega) = 1$) local density of states of reservoir l , $\rho_{c,l}^H(\omega)$ is its Hilbert transformed and $\rho_{c,l}^+(\omega)$ is proportional to the Keldysh component of the Green's function. Since the reservoirs are taken to be in equilibrium, the fluctuation dissipation theorem can be applied and it is found that

$$\rho_{c,l}^+(\omega) = f_l(\omega) \rho_{c,l}^-(\omega), \quad (\text{S.27})$$

with

$$f_l(\omega) = [1 - 2n_{f_l}(\omega - \mu_l)] = \tanh \left[\frac{\beta_l}{2} (\omega - \mu_l) \right]. \quad (\text{S.28})$$

Here, $n_{f_l}(\omega - \mu_l)$ is the Fermi-function, and β_l and μ_l are the inverse temperature and the chemical potential of reservoir l . The lead's Green's functions can thus be written in the form

$$\tilde{g}_c^{R,A}(\omega) = -\pi [\rho_c^H(\omega) \pm i\rho_c^-(\omega)], \quad (\text{S.29})$$

$$\tilde{g}_c^K(\omega) = -2\pi i\rho_c^+(\omega), \quad (\text{S.30})$$

with

$$\rho_c^-(\omega) = \frac{J_L \rho_{c,L}^-(\omega) + J_R \rho_{c,R}^-(\omega)}{J_L + J_R}, \quad (\text{S.31})$$

$$\rho_c^+(\omega) = \frac{J_L f_L(\omega) \rho_{c,L}^-(\omega) + J_R f_R(\omega) \rho_{c,R}^-(\omega)}{J_L + J_R}. \quad (\text{S.32})$$

Self-consistent equations for the steady-state

With the definitions of the previous sections, Dyson's equation translates to

$$\begin{aligned} \rho_f^\pm(\omega) &= \sigma_f^\pm(\omega) \left\{ \left[\omega - \tilde{\lambda} + \pi \sigma_f^H(\omega) \right]^2 + \left[\pi \sigma_f^-(\omega) \right]^2 \right\}^{-1}, \\ \rho_B^\pm(\omega) &= \sigma_B^\pm(\omega) \left\{ \left[-(J_L + J_R) + \pi \sigma_B^H(\omega) \right]^2 + \left[\pi \sigma_B^-(\omega) \right]^2 \right\}^{-1}, \end{aligned}$$

with $\tilde{\lambda} = \lambda_t - \frac{\kappa}{2} (J_L + J_R) \int d\omega \rho_c^+(\omega)$ being a renormalized chemical potential, and Eq.(S.22-S.24) translate to

$$\sigma_B^\pm(\omega) = \mp \frac{1}{2} \int d\nu \left[\rho_c^\pm(\nu - \omega) \rho_f^+(\nu) - \rho_c^\mp(\nu - \omega) \rho_f^-(\nu) \right], \quad (\text{S.33})$$

$$\sigma_f^\pm(\omega) = \kappa \frac{1}{2} \int d\nu \left[\rho_c^\pm(\omega - \nu) \rho_B^+(\nu) + \rho_c^\mp(\omega - \nu) \rho_B^-(\nu) \right], \quad (\text{S.34})$$

$$q = \frac{1}{2} \left[1 - \int d\omega \rho_f^+(\omega) \right]. \quad (\text{S.35})$$

In the particle-hole symmetric case ($q = 1/2$) and for a particle-hole symmetric DOS of the leads ($\rho_c^-(\omega) = \rho_c^-(-\omega)$) the quantities $\rho_{f,B}^\pm$ and $\sigma_{f,B}^\pm$ are real.

Details of the numerical treatment

The explicit form of the pseudogap density of states of the leads is taken to be

$$\rho_{c,l}^-(\omega) = \frac{1}{\sqrt{2}\Lambda \Gamma\left(\frac{r+1}{2}\right)} \left| \frac{\omega}{\sqrt{2}\Lambda} \right|^r e^{-\frac{\omega^2}{2\Lambda^2}},$$

with $l = R, L$ and $\Lambda = 1$ specifies the soft high-energy cutoff. The self-consistent equations were solved iteratively on a logarithmically discretized grid with 350 points ranging from -10Λ to 10Λ . The criterium for convergence of the selfconsistency loop was that the relative difference of two consecutive iterations was less than 10^{-6} . The results were benchmarked by the conditions that the fluctuation dissipation ratios of the Green's functions have to accurately reproduce the equilibrium fluctuation dissipation relations demanded by the fluctuation-dissipation theorem.

Observables

Cross 4-point function

In order to compute the currents and the Kondo singlet strength we will need to evaluate the connected 4-point function $\langle T_\gamma c_{p_2\alpha_2\sigma_2l_2}^\dagger c_{p_1\alpha_1\sigma_1l_1} f_{s_2}^\dagger f_{s_1} \rangle_C$. Here, C denotes the connected part of a correlation function and T_γ is the time-ordering operator on the Keldysh contour. Using the procedure outlined above, one obtains

$$\langle T_\gamma f_{s_1}(t_1) f_{s_2}^\dagger(t_2) c_{p_1\alpha_1\sigma_1l_1}(t_3) c_{p_2\alpha_2\sigma_2l_2}^\dagger(t_4) \rangle_C = i \frac{1}{N} \frac{1}{n_c} \delta_{s_1\sigma_2} \delta_{s_2\sigma_1} \delta_{\alpha_1\alpha_2} F_{p_1l_1;p_2l_2}(t_1, t_2, t_3, t_4)$$

and

$$F_{p_1l_1;p_2l_2}(t_1, t_2, t_3, t_4) = \frac{\sqrt{J_{l_2}J_{l_1}}}{\sqrt{(J_L + J_R)(J_L + J_R)}} \times \int dz' \int dz G_f(t_1, z) g_{c;p_2l_2}(z, t_4) G_B(z, z') g_{c;p_1l_1}(t_3, z') G_f(z', t_2)$$

with $g_{c;p_1l_1}(t, t') = \langle t p_1 l_1 | g_c | t' p_1 l_1 \rangle$. For equal times we have

$$\langle c_{p_2\alpha_2\sigma_2l_2}^\dagger(t) c_{p_1\alpha_1\sigma_1l_1}(t) f_{s_2}^\dagger(t) f_{s_1}(t) \rangle_C = i \frac{1}{N} \frac{1}{n_c} \delta_{s_1\sigma_2} \delta_{s_2\sigma_1} \delta_{\alpha_1\alpha_2} F_{p_1l_1;p_2l_2}(t),$$

where the time-ordering for the equal-time limit is defined through $F_{p_1l_1;p_2l_2}(t) = \lim_{t_1, 2, 3, 4 \rightarrow t} F_{p_1l_1;p_2l_2}(t_1, t_2, t_3, t_4)|_{t_1 > t_2 > t_3 > t_4}$. $F_{p_1l_1;p_2l_2}(t)$ can be explicitly evaluated using Langreth rules and making use of the fact that we describe a steady-state. This procedure is straightforward but involved and yields

$$F_{p_1l_1;p_2l_2}(t) = 4i\pi^5 \left[\mathcal{I}_{l_1p_1, l_2p_2}^{(1)} + \mathcal{I}_{l_1p_1, l_2p_2}^{(2)} \right],$$

with

$$\begin{aligned} \mathcal{I}_{p_1, p_2}^{(1)} &= \frac{1}{8} \frac{\sqrt{J_{l_2}J_{l_1}}}{(J_L + J_R)} \int \frac{d\omega}{2\pi} \{ [-i\mathcal{H}[A_{l_2}^{++++}](\omega) + A_{l_2}^{++++}(\omega)] [2\rho_B^+(\omega)] [i\mathcal{H}[A_{l_1}^{++++}](\omega) + A_{l_1}^{++++}(\omega)] \\ &\quad + [-i\mathcal{H}[A_{l_2}^{++--}](\omega) + A_{l_2}^{++--}(\omega)] [-i\rho_B^H(\omega) + \rho_B^-(\omega)] [i\mathcal{H}[A_{l_1}^{++--}](\omega) + A_{l_1}^{++--}(\omega)] \\ &\quad + [-i\mathcal{H}[A_{l_2}^{--++}](\omega) + A_{l_2}^{--++}(\omega)] [i\rho_B^H(\omega) + \rho_B^-(\omega)] [i\mathcal{H}[A_{l_1}^{--++}](\omega) + A_{l_1}^{--++}(\omega)] \} \\ \mathcal{I}_{p_1, p_2}^{(2)} &= \frac{1}{2} \sqrt{J_{l_2}J_{l_1}} \frac{1}{2\pi i} \int \frac{d\omega}{2\pi} \{ [-i\mathcal{H}[A_{l_2}^{++++}](\omega) + A_{l_2}^{++++}(\omega)] A_{l_1}^{--++}(\omega) \\ &\quad - [-i\mathcal{H}[A_{l_2}^{--++}](\omega) + A_{l_2}^{--++}(\omega)] A_{l_1}^{++--}(\omega) \}, \end{aligned}$$

where we defined

$$\begin{aligned} A_l^\Sigma(\omega) &= \int \frac{d\nu}{2\pi} \left[\rho_f^{\Sigma(1)}(\nu) \rho_{c, p_l}^{\Sigma(2)}(\nu - \omega) - \rho_f^{\Sigma(3)}(\nu) \rho_{c, p_l}^{\Sigma(4)}(\nu - \omega) \right], \\ \mathcal{H}[A](\omega) &= -\frac{1}{\pi} P \int d\nu \frac{A(\nu)}{\omega - \nu}. \end{aligned}$$

Currents

The currents of particles and energy through the system are obtained from the change in particle number and energy of *e.g.* the left lead through a continuity equation for the conserved charge (particle number or energy),

$$\begin{aligned} \mathcal{J}_b &= -\partial_t \langle \mathcal{Q}_b(t) \rangle = -i \langle [H(t), \mathcal{Q}_b(t)] \rangle \\ \mathcal{J}_E \rightarrow \mathcal{Q}_E &= H_L = \sum_{p, \alpha\sigma} \varepsilon_{pL} c_{p\alpha\sigma L}^\dagger c_{p\alpha\sigma L} \\ \mathcal{J}_P \rightarrow \mathcal{Q}_P &= N_L = \sum_{p, \alpha\sigma} c_{p\alpha\sigma L}^\dagger c_{p\alpha\sigma L} \end{aligned}$$

Using the identity $[c_\alpha^\dagger c_\beta, c_\gamma^\dagger c_\delta] = \delta_{\beta,\gamma} c_\alpha^\dagger c_\delta - \delta_{\alpha,\delta} c_\gamma^\dagger c_\beta$ and the fact that the Hamiltonian can be decomposed as $H = H_L + H_R + H_J$ with

$$H_J = \frac{1}{N} \sum_{ll'} J_{ll'} \sum_{\sigma\sigma'} \sum_{\alpha} (f_\sigma^\dagger f_{\sigma'} - q \delta_{\sigma\sigma'}) c_{0,\alpha\sigma'l'}^\dagger c_{0\alpha\sigma l},$$

one obtains

$$\begin{aligned} \mathcal{J}_P(t)/M &= 2\sqrt{J_{L,t}J_{R,t}} \operatorname{Re} \left[\frac{1}{n_c^2} \sum_{pp'} F_{Rp',Lp}(t) \right], \\ \mathcal{J}_E(t)/M &= 2\sqrt{J_{L,t}J_{R,t}} \operatorname{Re} \left[\frac{1}{n_c^2} \sum_{pp'} \varepsilon_{pL} F_{Rp',Lp}(t) \right]. \end{aligned}$$

Susceptibility

On the Keldysh contour the impurity spin susceptibility is defined by

$$\chi(z, z') = -i \frac{1}{N} \sum_a \langle T_\gamma S^a(z) S^a(z') \rangle,$$

where T_γ is the time-ordering operator on the Keldysh contour.

For a steady state, we obtain

$$\chi^\pm(\omega) = -\frac{1}{2} \int d\nu \left[\rho_f^+(\nu - \omega) \rho_f^\pm(\nu) - \rho_f^-(\omega - \nu) \rho_f^\mp(\nu) \right],$$

where $\chi_f^\pm(\omega) = -\frac{1}{2\pi i} [\chi^>(\omega) \pm \chi^<(\omega)]$.

Kondo singlet strength

It follows from the Hamiltonian, Eq. (1), that the Kondo term contribution to the total energy is given by

$$\begin{aligned} E_K(t) &= \frac{1}{N} \sum_{ll'} \sum_c J_{ll'} \langle \mathbf{S}(t) \cdot \mathbf{s}_{c,ll'}(t) \rangle \\ &= \kappa \left(\frac{N^2 - 1}{N} \right) \left\{ i \sum_{l_1 l_2} J_{l_1 l_2} \left[\frac{1}{n_c^2} \sum_{p_1 p_2} F_{p_1 l_1; p_2 l_2}(t) \right] \right\} \\ &= -J\kappa \left(\frac{N^2 - 1}{N} \right) \phi_s(t). \end{aligned}$$

This expression can be greatly simplified using the definition of $F_{p_1 l_1; p_2 l_2}(t)$, see previous section. This then yields for the Kondo singlet strength

$$\phi_s = \pi/J w^H(0),$$

with

$$w^-(\omega) = \frac{1}{2} \int d\nu [\sigma_B^+(\nu - \omega) \rho_B^-(\nu) - \sigma_B^-(\nu - \omega) \rho_B^+(\nu)].$$

Additional numerical results

In this section we provide further numerical support for our conclusions. Figure S1 shows our results for the parameter set $(r, \kappa) = (0.15, 0.16)$ which is different from the one the results in the paper are based on.

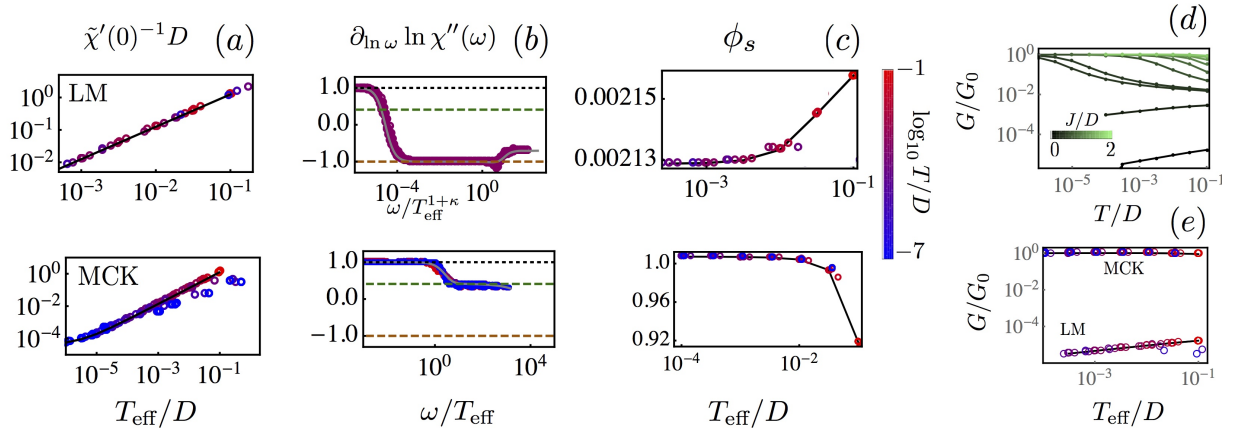


Figure S1. Scaling of different observables with T_{eff} for the different fixed points (the parameters used here differ from those of Figure 3 and 4 of the paper): (a) Inverse static susceptibility $\chi'(0)^{-1}$ vs T_{eff} ; (b) $\partial_{\ln \omega} \ln \chi''(\omega)$ vs ω/T_{eff} ; (c) singlet strength ϕ_s vs T_{eff} . For each fixed point, the equilibrium scaling form (black dashed lines) is compared with the same quantity under non-equilibrium conditions where T is substituted by T_{eff} . (d) Conductance G as a function of temperature computed for the lowest non-zero value of V for several values of J (see color coding). (e) $G = \mathcal{J}_P/V$ vs T_{eff} for the different fixed points. The equilibrium form is depicted by the black dashed lines. G_0 is defined as the zero-temperature limit of G in the MCK regime.